ADVANCED ALLOY DESIGN TOOLS APPLIED TO THE DEVELOPMENT OF VANADIUM NITRIDE STRENGTHENED HIGH-TEMPERATURE STEELS

D. Gaude-Fugarolas[1*] V. Yardley[1,3] J-M. Lardon[2] J. Montagnon[2]
Y. De Carlan[1]

1.- CEA Saclay
SRMA/LA2M bât 453
91191 Gif Sur Yvette CEDEX (France)
2.- Aubert et Duval
Parc Technologique La Pardieu 6 r Condorcet
63063 Clermont Ferrand CEDEX 1 (France)
3.- Now at Tohoku University (Japan)

Abstract

The modern power generation industry is constantly seeking to attain higher efficiency levels to obtain better environmental and economic performance. In order to achieve these goals, materials are needed with sufficiently high creep resistance to withstand operation under more demanding conditions, particularly higher service temperatures. A new generation of Fe8-12Cr ferrito-martensitic steels have the potential to become optimal candidates for various critical applications in the thermal and nuclear power generation and petrochemical industries.

One effective method of enhancing the creep resistance of an alloy is by producing a fine precipitate distribution that minimises deformation at service temperatures. MX precipitates such as VN are especially suitable for this task, due to their morphology, homogeneous distribution and slow coarsening (especially in comparison with $M_{23}C_6$-type carbides). Moreover, VN is stable to higher temperatures than $M_{23}C_6$, allowing an increase in the working temperature of the alloy.

An alloy with a high nitrogen content is not devoid of potential problems, and therefore careful design of the alloy composition and heat treatments are needed. The occurrence of porosity related to high nitrogen content has been noted. The maximum nitrogen content (both in absolute terms and relative to other elements, e.g. V/N, V/C) needs to be optimised in order to obtain the best possible mechanical performance whilst minimising the risk of porosity after casting.

In the work described here, thermodynamic software packages based on the CALPHAD method, together with advanced statistical analysis using neural networks, were used to suggest optimum compositions, microstructures and heat treatments to obtain improved creep properties in a new set of alloys for the nuclear power industry. The computational work was complemented by the use of experimental castings and characterisation of a selection of alloys of various compositions and with a wide range of nitrogen contents. This also enabled the development of a criterion to predict the

*Corr. Author: dgaude@cantab.net Tel: +33 (0)1 69 08 22 69 Fax: +33 (0) 169 08 71 30

formation of nitrogen-induced porosity during casting; this should be useful both to research and to the steel-making industry.

Keywords: Cr-Steel; Creep; VN Precipitation; Porosity; Neural Networks

Introduction

In order to satisfy more demanding efficiency requirements and to achieve better environmental and economic performance, the modern power generation industry requires a continuous process of improvement. New materials able to outperform present ones in safety, mechanical properties and service temperature are a continuous need in this process. In the past, the process of designing a new material was mostly heuristic, requiring repeated experimental trial and error, but the accuracy of current scientific knowledge in thermodynamics and transformation kinetics enables us to design successful new alloys using minimal empirical feedback. The design process is, however, still somewhat iterative, each stage leading to a more refined definition of the final alloy. The difference from the traditional approach is that most of the process is performed theoretically or computationally, involving the production of only a few essential trial casts to verify the suitability of the product material.

Design methodology and discussion

To illustrate the potential of modern materials design methods, a new family of alloys for the nuclear power industry has been developed. Ferritic-martensitic steels are known to perform well as low-activation materials, due to their low swelling under radiation and long service life at high temperatures [1]. An Fe8-12Cr ferritico-martensitic alloy was selected as the basis for this new type of alloy, due to its good balance between mechanical properties and oxidation resistance [1, 2, 3]. A neural-network model based on a large database of creep properties of alloys used in high-temperature applications was then used to narrow the range of suitable compositions. An alloy containing carbon, chromium, tungsten, vanadium and nitrogen was chosen.

Creep damage involves several competing mechanisms, but under typical power plant conditions, the main mechanism consists of the easy glide of dislocations along slip planes, and the subsequent, thermally activated dislocation climb into a different slip plane when dislocations encounter an obstacle (for instance, an incoherent precipitate). Providing a fine distribution of precipitates that remain stable at service temperature is therefore a suitable strategy to improve the creep behaviour of an alloy [4].

The composition selected provides the possibility of reinforcing the microstructure with a nanometric distribution of MX-precipitates. VN precipitates, for instance, are stable at higher temperatures than other MX precipitates or $M_{23}C_6$ carbides, and are less prone to coarsening than $M_{23}C_6$ [2, 5]. Calculations of the stability of phases were performed using thermodynamic models based on the CALPHAD method [6, 7]. When dealing with high nitrogen contents, there is a risk of developing a small amount of porosity in the material. Sometimes this kind of problem is not obvious at the first stages of the process of alloy design, but it clearly needs to be taken into account nonetheless. Obviously, there is a demand to find suitable criteria that could be applied in research and industrial environments to predict the occurrence of such porosity. One such criterion for the occurrence of porosity in high-nitrogen alloys is presented in this work.

The optimal heat treatment to obtain the desired distribution of precipitates in a suitable microstructure was determined using a thermodynamic and kinetic model based on the CALPHAD method and the

Onsager extremum principle [8, 9, 10]. The alloy designed in this way was cast at the *Aubert et Duval* steelworks and its properties are being characterised at CEA Saclay.

General composition

Many alloys for high temperature applications, especially in the power generation industry, are based on the Fe8-12Cr system. This family of alloys presents a good compromise between mechanical properties (especially creep resistance) and oxidation resistance [1, 2, 3]. The optimal structures for high temperature nuclear applications are the body-centred cubic ferritic or martensitic phases, usually as a matrix with a complex arrangement of reinforcing precipitates. Austenitic alloys lack the capability of ferritic alloys of withstanding the radiation damage, especially swelling [1, 2, 3].

A balance between ferrite-stabilising (or α-gen) elements and austenite-stabilising (or γ-gen) elements needs to be achieved in the alloy composition to avoid the formation of δ-ferrite at the austenitisation temperature. This phase would produce brittleness in the final component, and unless the structure could be fully transformed into austenite, the subsequent transformation to martensite on quenching would be incomplete [3, 11].

Some alloying elements, such as Mo, Ni, Nb, Si, Mn, Co and B, which are commonly used to improve the properties of steels for the conventional power generation industry and other high-temperature applications, need to be reduced or even excluded entirely from alloys intended for use in the nuclear industry because of their behaviour under neutron irradiation. They are commonly substituted by W, V and Ta in alloys intended for operation under radiation [1, 2, 3].

Starting from the general criteria found in the literature, a first set of compositions was defined, and then a thermodynamic calculation software package was used to select the ones that would fit to the microstructure requirements imposed. The thermodynamic software packages MTDATA and Thermocalc were used to perform this type of calculation on the thermodynamic stability of the phases of interest [3, 11]. A general range of possible compositions including the elements Fe, Cr, W, V, N, and C but with limited contents of Ni, Si, Mn and B was therefore selected following the above criteria.

At the same time, and in order to analyse the effect of small variations of each element on the creep resistance of the alloy (and the respective interactions), an advanced statistical method was used, a Bayesian-based neural network [12, 13]. Cole *et al.* had trained a neural network describing the creep properties of a wide range of steels [14]. This model is publicly available at the Materials Algorithms Project website [15]. Using this tool, the effect of variations in composition on the creep rupture strength after 100,000 hours was analysed and a well-defined composition was defined that would potentially maximise creep resistance.

In all figures showing the predictions obtained with the neural network model (Figures 1 to 6), the predictions for each set of conditions are plotted in solid lines and surrounded by dashed lines representing the *errorbar* or confidence estimate of the prediction [12, 13].

According to the predictions using the neural network trained by Cole *et al.* [14], for some elements there was an optimal composition range (represented by a maximum in the predicted creep rupture strength at 10,000 hours). This was the case for Cr and W, elements for which the optimal contents were around 9.5 wt.% (Figure 1) and 2 wt.% (Figure 3) respectively. In the case of chromium, this value lies in the lower end of the range of compositions traditionally used for high-temperature applications, and therefore it will be necessary to pay special attention to aspects such as the corrosion resistance of the alloy. Tungsten is usually added to produce solid solution strengthening of the matrix, but it is also a strong α-gen element.

Carbon has a strong solid solution strengthening effect, and according to the neural network predictions (Figure 2), the creep rupture strength of the alloy increases monotonically with its carbon content.

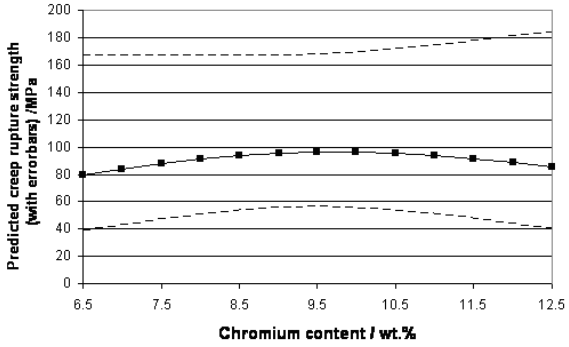

Figure 1: Creep rupture strength predicted using a neural network as a function of chromium content.

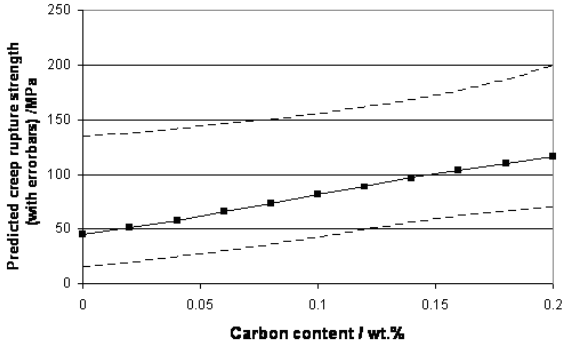

Figure 2: Creep rupture strength predicted using a neural network as a function of carbon content.

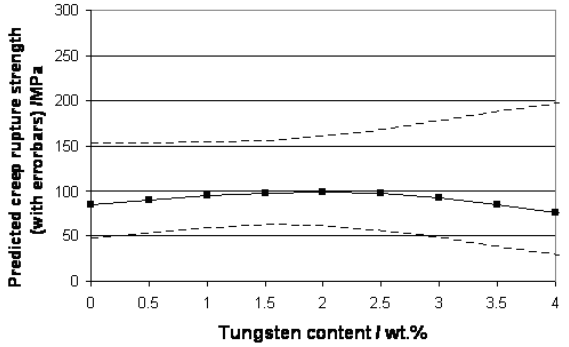

Figure 3: Creep rupture strength predicted using a neural network as a function of tungsten content.

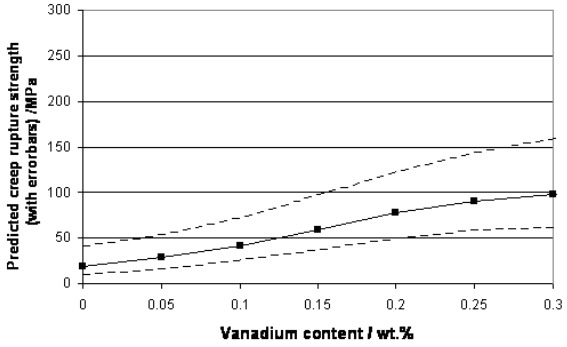

Figure 4: Creep rupture strength predicted using a neural network as a function of vanadium content.

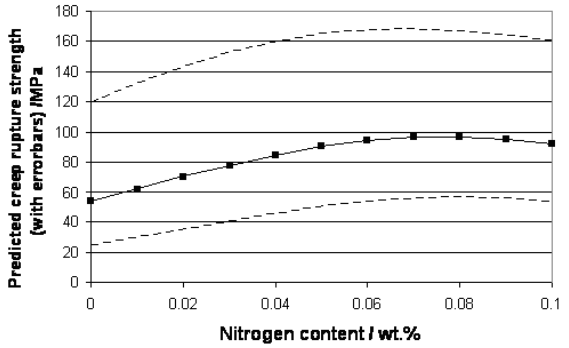

Figure 5: Creep rupture strength predicted using a neural network as a function of nitrogen content.

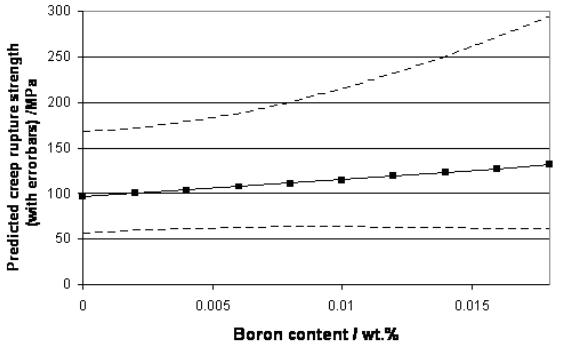

Figure 6: Creep rupture strength predicted using a neural network as a function of boron content.

Carbon is also a strong γ-gen element, which helps to compensate for the increase in α-gen elements such as W or V. However, this trend needs to be treated with caution, as not all the carbon stays in solid solution; instead it tends to precipitate as $M_{23}C_6$. $M_{23}C_6$ precipitates have rapid coarsening kinetics and therefore produce little improvement in the mechanical properties. In addition, they 'steal' Cr from the matrix of the alloy, reducing its oxidation resistance. Better results are expected from a fine distribution of MX precipitates (*i.e.* VN), which not only coarsen more slowly, allowing for a potential improvement in creep resistance and toughness, but are also stable at higher temperatures. VN precipitates are able to play that strengthening role, and so it would seem at first to be advantageous to increase the content in both V and N. Indeed, the creep rupture strength increases with the vanadium content (Figure 4) but this element is at the same time a strong α-gen element, and an excess of it would prevent the complete austenitisation of the alloy. The predictions of the neural network suggest that the optimal nitrogen content lies around 0.07wt.%, as shown in Figure 5, but an excessive N content could lead to porosity in the cast, as will be described in a later section [11, 5].

Last but not least, Figure 6 shows that the predicted creep rupture strength increases with boron content. Even small additions of boron have an important influence on the creep behaviour of Cr-steels, as it diffuses to the surfaces of $M_{23}C_6$ precipitates, especially to those close to prior austenite grain boundaries, and slows down their coarsening [16, 17]. In the natural form of boron, the isotope B^{10} predominates. This has a deleterious effect in alloys exposed to irradiation, because it transforms to helium. However, since only small amounts of boron are necessary for improved creep properties, the less common isotope B^{11}, which does not exhibit this problem, could be isolated and used in alloys for nuclear applications, so that the beneficial effect of boron could still be obtained [11].

To conclude, after examining the related literature and analysing the possible compositions with the help of advanced statistical methods, an alloy composition optimised to maximise the creep rupture strength, while presenting good oxidation properties, was chosen. The proposed composition was (all compositions are in wt.%) Fe 9.5Cr 0.14C 2.5W 0.35V with up to 0.07N and with the possibility of small (less than 0.1 wt.%) additions of B^{11}.

Microstructure and heat treatments

Once the composition of the alloy has been selected, the heat treatments to obtain the desired microstructure need to be carefully designed. In order to obtain the fine precipitation of vanadium nitrides we need first to austenitise the alloy and dissolve all existing precipitates. Then one or more annealing treatments will allow the precipitation of VN in the austenitic matrix. Subsequent quenching to transform the austenite matrix to martensite and tempering to relieve internal stresses and to precipitate $M_{23}C_6$ and therefore to stabilise the microstructure will finish the treatment. Using a thermo-mechanical treatment would also be feasible, adding stages of hot rolling prior to annealing to increase the density of precipitate nucleation sites and hence to accelerate the precipitation reaction and reduce the average size of the precipitates. The optimisation of the heat treatment parameters (temperature and duration of each stage of the heat treatment) is possible using a software package such as 'MatCalc' developed by TU Graz, Austria, which combines equilibrium phase stability calculations with simulations of the kinetics of precipitation, (nucleation, growth and coalescence of precipitates), and predictions of the size distribution obtained with each set of conditions [8, 9, 10]. The package uses thermodynamic, mobility and physical property databases expressed in a standard CALPHAD-type format. The calculations for the present work were made using the database "IWS_Steel", developed at TU Graz.

Figure 7 shows the calculated phase stability diagram as a function of temperature for steel VY1. Using this diagram we can define the temperatures for the different stages of the heat treatment to obtain the optimal microstructure.

Using Figure 7 as a reference, we can define the austenitisation temperature at 1175°C, and then a

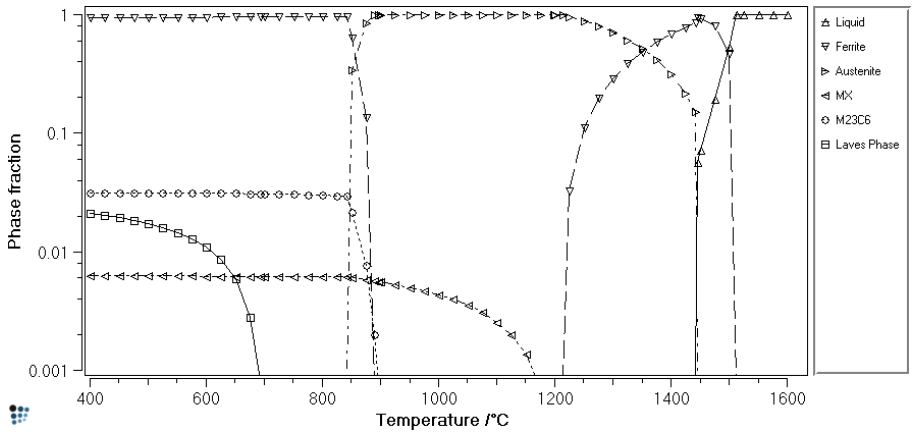

Figure 7: Phase distribution as a function of temperature for designed alloy. Diagram calculated using MatCalc.

subsequent annealing at 900°C for 1 hour to produce a distribution of VN precipitates. At this temperature, the driving force for precipitation of vanadium nitrides is large and the equilibrium phase fraction of precipitates is close to the maximum it is possible to reach at any temperature. Parameters such as austenite grain size and dislocation density could be modified to account for different starting conditions of recrystallisation, grain size and hot work. In the example shown in Figures 8 to 10 an austenite grain size of 100 μm and two different dislocation densities, representing annealed and hot worked microstructures, have been used. After the MX-precipitation annealing, the alloy should be quenched to transform austenite to martensite and finally a last stage of stabilisation tempering is performed at 700°C for 3 hours to reduce internal stresses and to precipitate $M_{23}C_6$.

Using a software package that includes at the same time thermodynamics and precipitation and coarsening kinetics simplifies considerably the selection of optimal heat treatment conditions to obtain the desired microstructure and precipitate distribution, while avoiding incomplete precipitation reactions or excessive precipitate coarsening. In the present case, the duration of the MX precipitation annealing is chosen to ensure that the equilibrium fraction of MX has been reached. On Figures 8 to 10 we see that 30 minutes would suffice but an hour has been chosen to ensure that reaction is complete but that there is no significant coarsening. The same procedure is applied to the stabilisation annealing and the precipitation of $M_{23}C_6$. The final distribution of reinforcing phases predicted comprises in both cases coarser particles of $M_{23}C_6$ than MX, but the effect of the initial density of dislocations (and therefore of nucleation sites) makes a large difference in the scale of MX precipitates. A similar calculation could be performed to study the evolution of the microstructure during service conditions, for instance to predict the excessive coarsening of some of the reinforcing phases or to anticipate deleterious phases that have very slow kinetics, like Z-phase.

Undesirable phase: Nitrogen gas

As the nitrogen content of the alloy is increased to produce a larger extent of precipitation of the reinforcing phase VN, there is an increased risk that the matrix of the alloy will not be able to keep in solution all the nitrogen and some will be released as gas, resulting in the formation of porosity. Some alloys with very high nitrogen content can even present macroscopic porosity, as shown in Figure 11. The nitrogent content of the alloy shown in Figure 11 is 0.073wt.% .

Some Cr-steels with substantial nitrogen contents develop porosity (*e.g.* the alloy designated A2, in

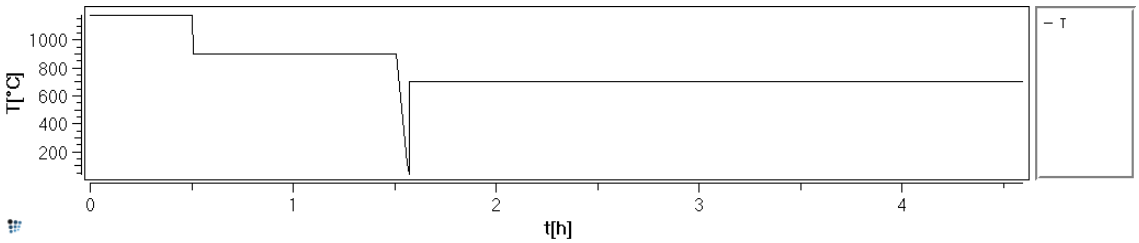

Figure 8: Simulated heat treatment on the designed alloy: Fe9.5Cr0.14C2.5W0.35V0.07N (wt.%).

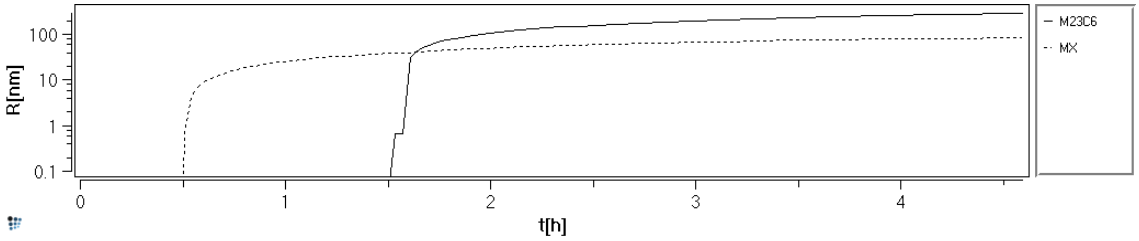

Figure 9: Simulation of the evolution of the average radius of MX and $M_{23}C_6$ precipitates on the designed alloy with dislocation density in austenite of $10^{11}\mathrm{m}^{-2}$ and in martensite of $10^{14}\mathrm{m}^{-2}$ (*i.e.* as annealed).

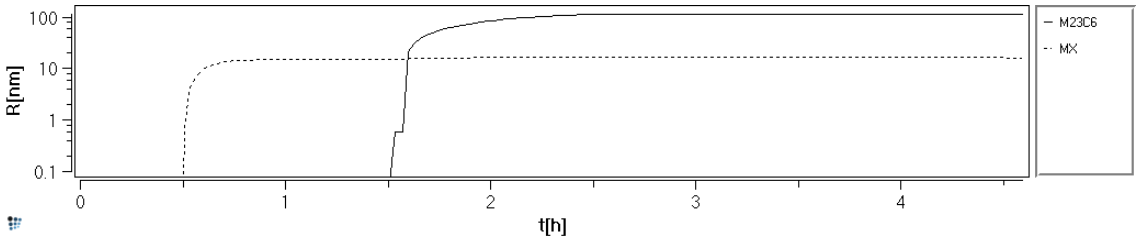

Figure 10: Simulation of the evolution of the average radius of MX and $M_{23}C_6$ precipitates on the designed alloy with dislocation density in austenite of $10^{14}\mathrm{m}^{-2}$ and in martensite of $10^{15}\mathrm{m}^{-2}$ (*i.e.* as hot worked).

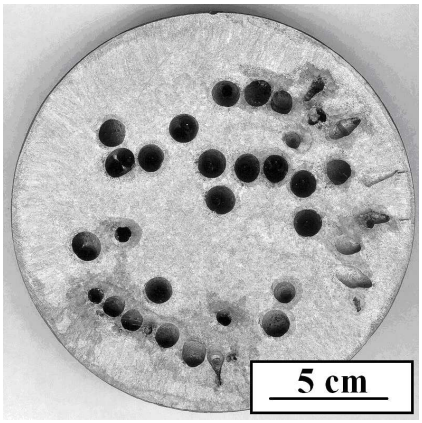

Figure 11: 'A2' steel showing nitrogen-induced porosity (in wt.% Fe 7.9Cr 0.1C 2.5W 0.3V 0.005Nb 0.073N).

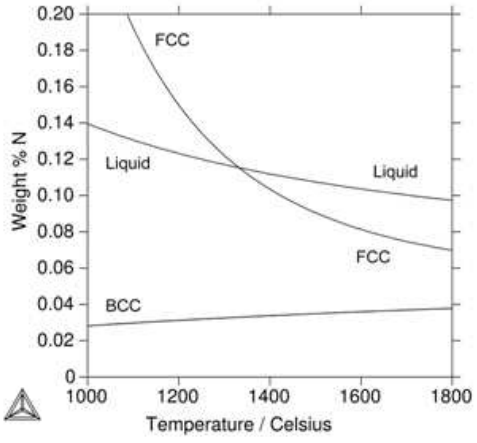

Figure 12: Nitrogen solubility limit for liquid, δ-ferrite, and austenite equilibrium with nitrogen gas, calculated using Thermocalc.

wt.% Fe 7.9Cr 0.1C 2.5W 0.3V 0.005Nb 0.073N), as shown in Figure 11, but others of similar composition do not (*e.g.* alloy T91, in wt.% Fe 8.24Cr 0.1C 0.43Si 0.37Mn 0.97Mo 0.2V 0.13Ni 0.075Nb 0.05N). The issue of porosity in the development of any industrial alloy is of severe importance as it can render an otherwise perfectly designed alloy completely useless. There is need to find a suitable criterion to find out which compositions are susceptible to porosity.

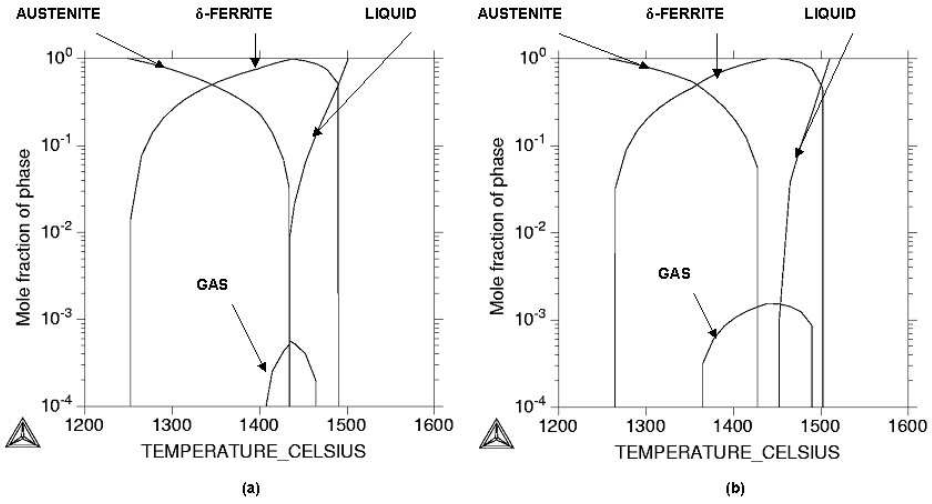

Figure 13: Phase stability diagrams for steels (a) T91 (in wt.% Fe 8.24Cr 0.1C 0.43Si 0.37Mn 0.97Mo 0.2V 0.13Ni 0.075Nb 0.05N) and (b) A2 (in wt.% Fe 7.9Cr 0.1C 2.5W 0.3V 0.005Nb 0.073N), showing the thermodynamic stability of the gas phase and the different equilibrium transformation path in each case.

The phase diagrams as a function of temperature of the two alloys mentioned above, A2 and T91, are shown in Figure 13. These diagrams have been calculated using Thermocalc and its standard database TCFE3. It can readily be observed that in both cases the nitrogen gas is predicted to be a stable phase. On the other hand, the series of transformation reactions from liquid to austenite under equilibrium conditions would follow a different route in each case. For the T91 alloy the transformation proceeds as [liquid + δ-ferrite] $\rightarrow$ [δ-ferrite + austenite(γ)]. In the case of alloy A2 however, the transformation traces a different path: [liquid + δ-ferrite] $\rightarrow$ [δ-ferrite] $\rightarrow$ [δ-ferrite + austenite(γ)]. The transformation path followed by the alloy presenting severe porosity has crossed a phase field containing only δ-ferrite, while in the other alloy there is always a second phase (either liquid or austenite) accompanying δ-ferrite.

The nitrogen solubility limits in each of the three phases liquid, δ-ferrite, and austenite have been calculated in equilibrium with nitrogen gas using Thermocalc (Figure 12). The maximum solubility of nitrogen in δ-ferrite is much lower than in the liquid phase or in austenite, and while in the case of alloy T91 the nitrogen partitioning from δ-ferrite can still be dissolved in the liquid phase or in austenite, this is not possible in the case of alloy A2, and therefore an excess of nitrogen will appear in the form of gas and create bubbles that become trapped in the matrix of the alloy. Moreover, as nitrogen and vanadium are increased in parallel in the alloy to produce a larger distribution of VN precipitates, and as vanadium is an α-gen element, the risk of producing an alloy presenting porosity problems increases twofold.

The limiting (maximum) amount of nitrogen that the alloy can contain in equilibrium conditions can be determined by calculating the minimum amount that the whole microstructure can dissolve at any one temperature (*i.e.* the *bottleneck* of keeping all nitrogen in solution). We can express that value as,

$$[N]^{alloy}_{max} = MIN\left([N]^{\delta}_{max} \cdot X^{\delta} + [N]^{Liq.}_{max} \cdot X^{Liq.} + [N]^{\gamma}_{max} \cdot X^{\gamma}\right)\{T\} \quad (1)$$

where X^i is the fraction of each phase (δ-ferrite, liquid and austenite) and $[N]^i_{max}$ is the maximum solubility of nitrogen in the alloy or in phase i, as a function of temperature T.

Nevertheless, the process of forming a gas bubble in the alloy is not immediate, and the effect of kinetics needs to be taken into account. The formation of gas porosity is not unlike other phenomena governed by nucleation and growth [18]. In this case, nitrogen and vacancies need to coalesce in sufficient quantity to nucleate a *"bubble-nucleus"*, with the creation of new gas/matrix interfaces, and subsequently this nucleus needs to be able to grow above a certain critical size, becoming energetically stable instead of redissolving again in the matrix. The difference with the classical nucleation and growth scenario, however, is that in this case there is a term related to the pressure of the gas in the bubble that will contribute to its overall energy. Consequently, and with respect to the criterion described by Equation 1, there will be a region where the nitrogen gas will remain dissolved in the matrix in metastable conditions. For instance, it would be feasible to keep in solution an amount of nitrogen larger than the minimum of $[N]_{max}$ but lower than most of the curve as long as it was only for a short time. Likewise, it could be possible to keep in solution for a long time an amount of nitrogen that was only marginally higher that that described by Equation 1.

All parameters in Equation 1 can be calculated using a CALPHAD-based thermodynamic software package. From this expression it is clear that an alloy which presents a δ-ferrite single-phase region will not tolerate nitrogen content much higher than 300ppm (Figure 12) without producing a porous cast. Alloys that do not form δ-ferrite or in which this phase is part of a dual microstructure with either liquid or austenite at all temperatures will be more tolerant to large nitrogen contents.

Conclusions

The work presented here is a case study on how the current accuracy of thermodynamic and kinetic calculations allow new alloys to be designed to respond to demanding operating conditions, while avoiding most of the experimental trial and error needed in the past. Software tools based on the CALPHAD method and various kinetic models are available, allowing the prediction not only of the feasibility of a target microstructure but also of its evolution during various heat treatments.

In the present study a new reduced activation ferritic/martensitic alloy has been designed that should be able to sustain service temperatures of 650°C. This alloy has been cast and treated and is being characterised microstructurally and in terms of mechanical properties.

Acknowledgements:

The authors are grateful to Ms. A. Petit and Mr. F. Vivier for their collaboration in the development of this work and to Prof. H. K. D. H. Bhadeshia and Dr. E. Kozeschnik for their invaluable advice on the use of the various methods employed in the present work.

References

[1] J. L. Séran, J-C. Brachet, and A. Alamo. Fast reactor cores, ferritic-martensitic steels for. In *Enciclopedia of Materials: Science and Technology*, pages 2863–2866. Elsevier Science Ltd., 2001.

[2] H. K. D. H. Bhadeshia. Design of heat resistant alloys for the energy industries. In *5th International Charles Parsons Turbine Conference*, pages 3–39, 2000.

[3] Y. De Carlan, M. Murugananth, T. Sourmail, and H. K. D. H. Bhadeshia. Design of new Fe-9CrWV reduced-activation martensitic steels for creep properties at 650°C. *Journal of Nuclear Materials*, 329-333:238–242, 2004.

[4] R. W. Hertzberg. *Deformation and fracture mechanics of engineering materials.* John Wiley & sons, inc., New York, 1996.

[5] V. A. Yardley and Y. de Carlan. Design criteria for high-temperature steels strengthened with vanadium nitride. *Journal of Phase Equilibria and Diffusion*, 27, 2006.

[6] D. A. Porter and K. E. Easterling. *Phase transformations in metals and alloys.* Chapman & Hall, London, 1981.

[7] N. Saunders and A. P. Miodownik. *CALPHAD, calculation of phase diagrams, a comprehensive guide.* Pergamon Press, Oxford, 1998.

[8] J. Svoboda, F. D. Fischer, P. Fratzl, and E. Kozeschnik. Modelling of kinetics in multi-component multi-phase systems with spherical precipitates I: Theory. *Materials Science and Engineering A*, A385:166–174, 2004.

[9] E. Kozeschnik, J. Svoboda, P. Fratzl, and F. D. Fischer. Modelling of kinetics in multi-component multi-phase systems with spherical precipitates II: Numerical solution and application. *Materials Science and Engineering A*, A385:157–165, 2004.

[10] E. Kozeschnik, J. Svoboda, and F. D. Fischer. Modified evolution equations for the precipitation kinetics of complex phases in multi-cmponent systems. *Computer Coupling of Phase Diagrams and Thermochemistry*, 28:379–382, 2004.

[11] V. A. Yardley and Y. De Carlan. Progress in fabrication of experimental 9cr steel compositions optimised for creep resistance, thermodynamic and statistical analysis and proposed solutions. Technical report, CEA (France), 2005.

[12] D. J. C. MacKay. Bayesian non-linear modelling with neural networks. In H. Cerjak, editor, *Mathematical modelling of weld phenomena 3*, pages 359–389. The Institute of Materials, London, 1997.

[13] D. J. C. MacKay. Probable networks and plausible predictions - a review of practical Bayesian methods for supervised neural networks. In http://wol.ra.phy.cam.ac.uk/mackay/.

[14] D. Cole, C. Martin-Moran, A. G. Sheard, H. K. D. H. Bhadeshia, and D. J. C. MacKay. Modelling creep rupture strength of ferritic steel welds. *Science and Technology of Welding and Joining*, 5:81–89, 2000.

[15] Materials Science and Metallurgy Department - University of Cambridge and National Physical Laboratory. *Materials Algorithms Project.* University of Cambridge, http://www.msm.cam.ac.uk/map/mapmain.html, 1995.

[16] T. F. Kelly, D. J. Larson, M. K. Miller, and J. E. Flinn. Three dimensional atom probe investigation of vanadium nitride precipitates and the role of oxygen and boron in rapidly solidified 316 stainless steel. *Materials Science and Engineering A*, A270:19–26, 1999.

[17] F. Abe, T. Horiuchi, M. Taneike, and K. Sawada. Stabilisation of martensitic microstructure in advanced 9Cr steel during creep at high temperature. *Materials Science and Engineering A*, A378:299–303, 2004.

[18] J. W. Christian. *Theory of transformations in metals and alloys, Part I.* Pergamon Press, Oxford, 1975.